

III. Air Sparging

Introduction and General Description

In the context of ground water remediation, air sparging refers to the process of injecting air into the saturated zone while carrying out vapor extraction in the vadose zone. As air passes through the saturated sediments, free product and adsorbed and absorbed contaminants will evaporate and be carried away with the injected air. The injected air is then recovered by the vapor extraction system. The reasons for carrying out air sparging were discussed in the Introduction: the procedure is relatively cheap and easy to implement; high subsurface temperatures still available at the TFF site would enhance the volatilization of hydrocarbons; and the injected air would enhance microbial action and biodegradation of hydrocarbons. Because of the last point, we did not have much concern about the possibility that some of the injected air would not be recovered, but there remained a concern that some contaminant could be moved outward away from the central extraction well area. For this reason, it was important to be able to track the movement of the injected air and quantify how much of it was recovered.

In concept, it is a simple process to add air sparging onto an existing vapor extraction system. All that is needed is an air compressor, as a source of high pressure air, and wells with suitable screened intervals for injection and extraction. In practice, however, it is often difficult to determine just where the injected air goes and what effect it really has on the recovery of VOCs. In addition to buoyancy, the pattern of air flow in the subsurface will be controlled by the subsurface permeability distribution and geometry of the matrix material (e.g., a dipping surface of a high/low permeability contact may control the direction of flow and where the injected air will reach the vadose zone).

Because of the above concerns, we chose to carry out two small air sparging applications to test our ability to track the fate of the injected air and to determine what effect air sparging can have on recovery of hydrocarbons in a regime of elevated subsurface temperatures and with the water table lowered to expose a saturated aquitard. Electrical resistance tomography (ERT) wells were in place at the TFF site, so we decided to use LLNL capabilities in this area to see how well we could track the movement of the injected air. In addition, we were fortunate to be able to draw on the expertise and experience of personnel of the LLNL Nuclear Chemistry Division, who have been using noble gas isotope trace gases to monitor underground nuclear tests for many years. By injecting gas of a known composition and concentration along with the injected air and monitoring the tracer gases, we can determine how much of the recovered vapor at a given location is coming from the injected air, what the input flow rate is, and, with frequent sampling, how long it takes for the injected air to reach a sample location. In addition, we planned to take frequent samples of vapor at the injection and extraction wells for hydrocarbon chemistry analysis so that we could monitor the effect of sparging on hydrocarbon recovery. Because of the relatively rapid movement of air compared to water in the subsurface, all of the analyses of chemistry and trace gases had to be carried out with as short a turnaround as possible so that we could adequately determine what was happening and adjust the operations accordingly. For this reason, the fact that all analyses were done in-house, by LLNL personnel, was a great benefit.

In addition to sampling vapor for trace gases, we also took water samples for trace gas analysis from a ring of wells surrounding the central TFF area about 2 weeks after the completion of the sparging. Different trace gas compositions (the percentages and isotopes of krypton and xenon are given below) were used for each sparging configuration. Because of these differences, we would be able to separate the effects of each application and be able to tell how much of the injected air was incorporated into the ground water and detected outside of the area where injection occurred. The water samples have not yet been analyzed as of the writing of this report, so we are unable to report on those results at this time.

Another available tool that we took advantage of at LLNL is computer modeling. A general-purpose finite-difference fluid flow code, called NUFT, was developed by J. Nitao of the Earth Sciences Division at LLNL. This code is designed to simulate coupled fluid flow and heat transfer problems in three dimensions. It can model vapor, water, and free-product flow in both the saturated and vadose zone. The calculations can also simulate electrical heating from down-hole electrodes and incorporated contaminant chemistry for comparing the relative effects of steam heating versus electrical heating. For this project, we utilized NUFT to simulate relatively simple aspects of air sparging, steam injection, and electrical heating. These simulations, which are described in Appendix 5, proved to be very helpful for providing insight into the various physical processes and helping us understand what happens during various types of remediation.

At the TFF site, the character of well completions, as well as other factors, limits our choices for injection/extraction geometry. Our choices of wells suitable for injection of air and vapor extraction are limited to the three central extraction wells and the ring of six steam injection wells used during the DUSDP. The desire to carry out ERT imaging during air injection limited us to the use of combinations of wells optimally located with respect to existing ERT image planes. The central vapor extraction wells, which are also used to pump ground water (see Section II), are screened over large intervals in both the vadose and saturated zones and thus cannot be used to inject air exclusively into the saturated zone. At the time the sparging took place, water levels in the extraction and injection wells had been considerably lowered due to the 24-h pumping operations described above; in some cases, water levels in the injection wells were below the top of the screened interval in the lower steam zone.

An additional important factor in this application is the geometry of the base of the clay aquitard, which lies between the upper and lower steam zones. We suspected that this clay zone could impede upward movement of air; but, because of heterogeneities, we were not sure how effective a barrier it would be. Beneath the central part of the TFF site, the clay layer generally slopes from the southeast toward the northwest (Fig. 11) so that injected air, if trapped beneath the clay zone, could be expected to move toward the east and southeast. Limitations in the well and ERT configurations dictated the choice of injection and extraction wells for the sparging. We could do nothing about the configuration of the clay zone.

For the first sparging application, air was injected into the lower steam zone in injection well GIW820 while vapor extraction was carried out at the central extraction wells (GEW808, GEW816, and GSW16). Vapor samples, for analysis of both hydrocarbon chemistry and tracer gases, were taken at the injection well and at the outlet of the extraction wells. During and following cessation of air injection at GIW820, we also monitored the vapor concentration at injection well GIW815. The base of the aquitard slopes downward from GIW820 to GIW815 (Fig. 11). In this case, air injection rates averaged slightly less than one-half that of the

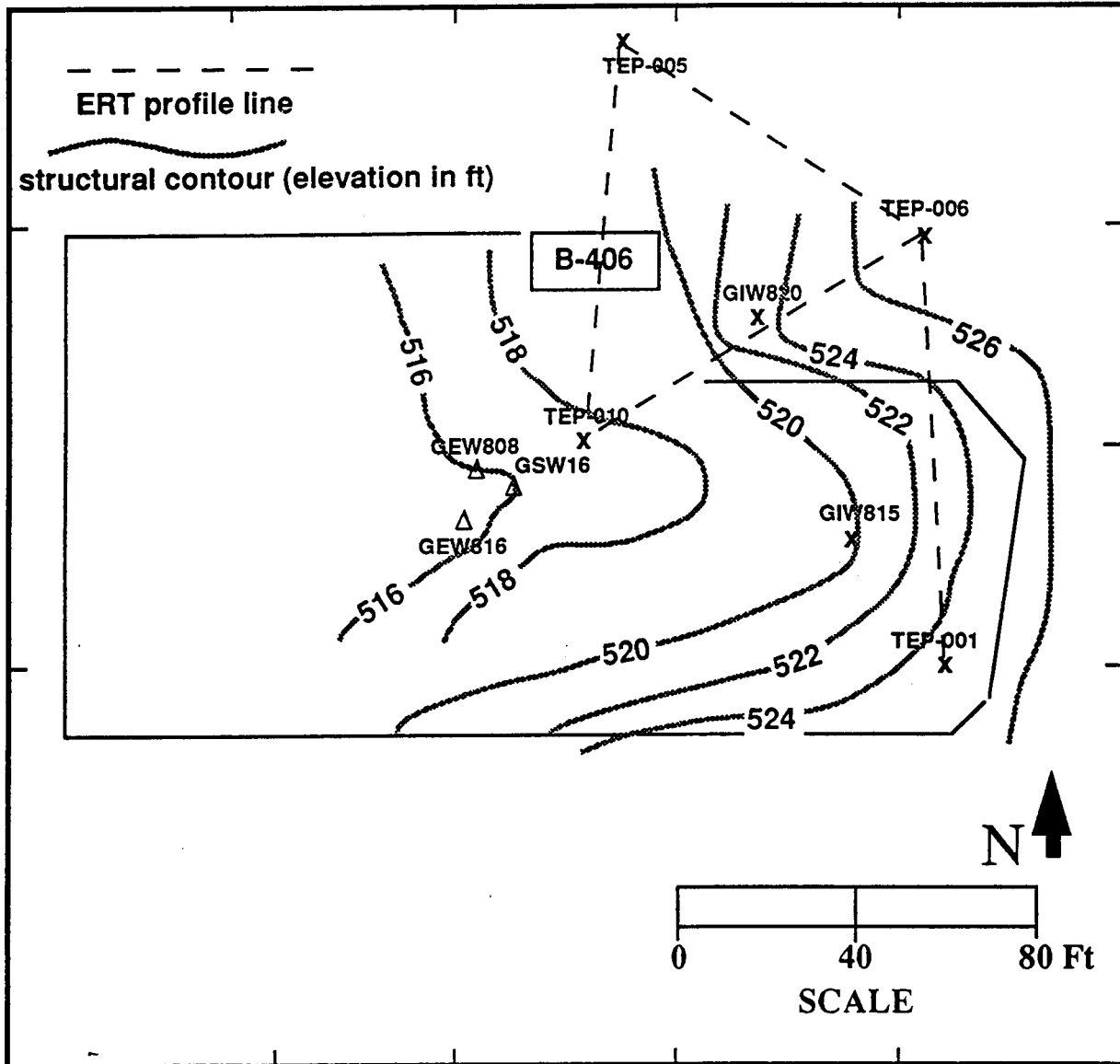


Figure 11. Location of wells and ERT profile lines used in the air sparging applications. Also shown are structure contours (elevation, in feet above mean sea level) of the base of the clay aquitard.

extraction rates. Within 5 h of the start of injection, we confirmed that most of the injected air was moving upslope to the east of wells GIW815 and GIW820, with only a very small part of the injected air being recovered by the extraction wells. Air injection was stopped after 7 h. Details of this application are given below.

The second sparging application was carried out one week after the first one, after vapor extraction conditions had been allowed to return to a stable level for reference. In this case, we injected air into well GIW815 and extracted vapor from well GIW820. Because the base of the aquitard at GIW820 is slightly upslope from where it is at GIW815, we presumed the air would have less of a geometric barrier to overcome and more of the injected air would be recovered. The injection rate in this case was about 0.8 times the extraction rate, and we eventually were able to recover about 45% of the injected air. A check of the water level in GIW815 after the air injection was stopped indicated that most of the air was injected in the vadose zone and not in the saturated zone as we had planned. Details are given below.

Air Sparging I

The first air sparging application took place November 16, 1993. An air compressor (modified with a conditioner to remove any oil or fuel from the output air) was attached to the steam injection manifold with connections to well GIW820. On November 8, vapor extraction was switched to the central extraction wells (GEW808, GEW816, GSW16) so that we could achieve a reliable background for reference on hydrocarbon removal from these wells prior to starting air sparging. The locations of the injection well, extraction wells, monitoring well GIW815 (see below), and the ERT profile planes are shown in Figure 11. Injected air flow rates were monitored by using calibrated measurements of absolute pressure and differential pressure, which gave us estimates of flow rates accurate to about 20%. The flow rate can also be monitored by sampling the composition of tracer gas in the air at the well head, as discussed below. Air was injected into the lower screened interval (112- to 132-ft depth) of well GIW820 beginning at 8:40 a.m. The initial pressure at the inlet steam manifold was 9 psi, gradually decreasing to a value of 6.6 psi when the compressor was shut off 7 h later. This initial injection pressure confirms that most of the air was being injected in the saturated zone. Injection rates, monitored at the input to the steam manifold every 30 min, were very constant at about 44 scfm. Extraction rates during the time of air injection were measured every 2 h at the ICE and ranged from 101 to 106 scfm.

For this sparging application, the trace gas composition was: ^{22}Ne , 0.68%; ^{78}Kr , 0.002%; ^{124}Xe , 0.000%; and air, 99.31%. The trace gases were injected at a rate of 1.0 L (STP)/min. Knowing the rate at which the trace gas was injected into the input air, we can determine the flow rate of the injected air via Figure 12. Measured values of the $^{22}\text{Ne}/^{20}\text{Ne}$ ratio at the input of the injection well ranged from 0.364 to 0.370, which corresponds to flow rates of 53 to 55 scfm. This value is about 15 to 20% higher than that estimated from the pressure gauges (see above), but well within the uncertainty of the pressure gauge measurements. The value of 53 to 55 scfm is probably more accurate.

Our intuitive concept of the air sparging process is that air injected into the lower steam zone in GIW820 would move buoyantly upward through the permeable sandy unit until it reaches the low-permeability clay zone that separates the upper and lower steam zones. Upon reaching this

The injected tracer dilution can calibrate the total flow (both applications).

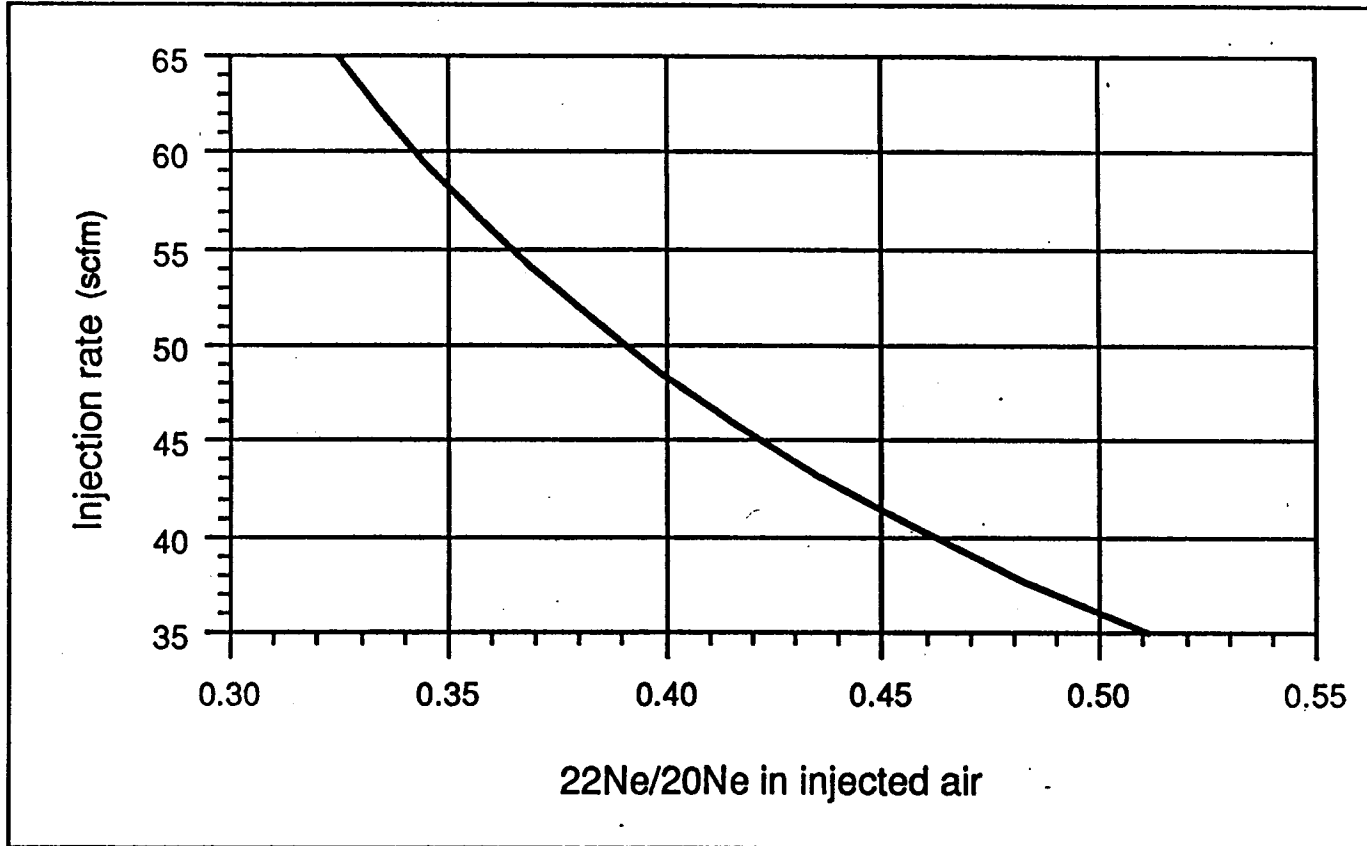


Figure 12. Calibration curve showing the relation between the air injection rate and the $^{22}\text{Ne}/^{20}\text{Ne}$ ratio in the injected air for the volumes of noble gas tracer mixture used in the air sparging applications.

barrier to upward movement, the air would move laterally, under the control of the slope on the base of the lower clay zone, until it reached some vertical discontinuity, such as a fracture or hydraulically conductive zone. This conductive pathway would allow the air to move upward into the vadose zone where it would come under the influence of the vapor extraction system. Using this concept and a cross section of the area between GIW820 and the extraction wells (Fig. 13), it appeared that the most likely path for the air was away (up, along the base of the confining zone) from the extraction wells. The gradient of the base of the clay zone is smaller to the south, so we decided to use GIW815 (Fig. 11) as a monitoring well to determine when and if injected air might pass in that direction.

These conceptual ideas were tested with a computer simulation, described in Appendix 5. The simulation suggested that most of the air would move toward the south and east, away from the extraction wells, and that none of the injected air would reach the extraction wells in the saturated zone. Without detailed knowledge of the subsurface heterogeneity, we could not be sure if possible "easy" paths to the vadose zone would affect the results. In addition, because the extraction wells are screened in both the vadose and saturated zones, we had no way to discriminate where the sampled air was coming from. The simulation also showed that the vapor extraction rate has little to no influence on the movement of air injected in the saturated zone. In order to have influence on the injected air comparable in any way to the buoyancy forces, we would have to pump ground water at the extraction wells at a volumetric rate greater than that of the air injection rate. This turned out to be a rate far in excess of the 50 gal/min rate of pumping the wells were capable of.

The trace gases were sampled approximately hourly at (1) the input to the injection well, (2) the input to the ICE (representing the composite of the vapor being extracted from the central extraction wells), (3) the lower steam zone interval of GIW815 (GIW815L) (112- to 132-ft depth), and (4) the upper steam zone interval of GIW815 (GIW815U) (77- to 97-ft depth). Vapor samples for noble gas tracers were taken by attaching an evacuated one-liter steel cylinder to the sampling port and opening the sampling port valve for 5 min. Depending on the flow rate of the input air, the $^{22}\text{Ne}/^{20}\text{Ne}$ ratio of the injected air varied from 0.364 to 0.370. Air recovered at various sampling points would have a $^{22}\text{Ne}/^{20}\text{Ne}$ ratio of 0.102, the background air value measured before the start of sparging, if none of the injected air was present. Values for the $^{22}\text{Ne}/^{20}\text{Ne}$ ratio above 0.102 meant that a portion of the injected air was present in the sample. The fraction of injected air in the sample can be calculated from:

$$F = [(22\text{Ne}/20\text{Ne})_{\text{meas}} - (22\text{Ne}/20\text{Ne})_{\text{air}}] / [(22\text{Ne}/20\text{Ne})_{\text{inject}} - (22\text{Ne}/20\text{Ne})_{\text{air}}]$$

where the subscripts refer to the Ne ratio measured in the sample, in background air, and in injected air, respectively. F is the fraction due to the tracer.

Table 2 shows the variation in the $^{22}\text{Ne}/^{20}\text{Ne}$ ratio versus time at the four sampling points. The flow rate at the injection well is determined from Figure 12. The percent injected air in the sample shown in Table 2 is the fractional value F times 100%. Note that GIW815 in this case was only being used as a monitoring well, and vapor was not being extracted from either the upper or lower steam interval. A vacuum hose was connected to each sampling port in GIW815 for 5 min each time before sampling in order to purge gas that accumulated between sampling intervals. Because there was no continuous flow in GIW815, these trace gas values can only be

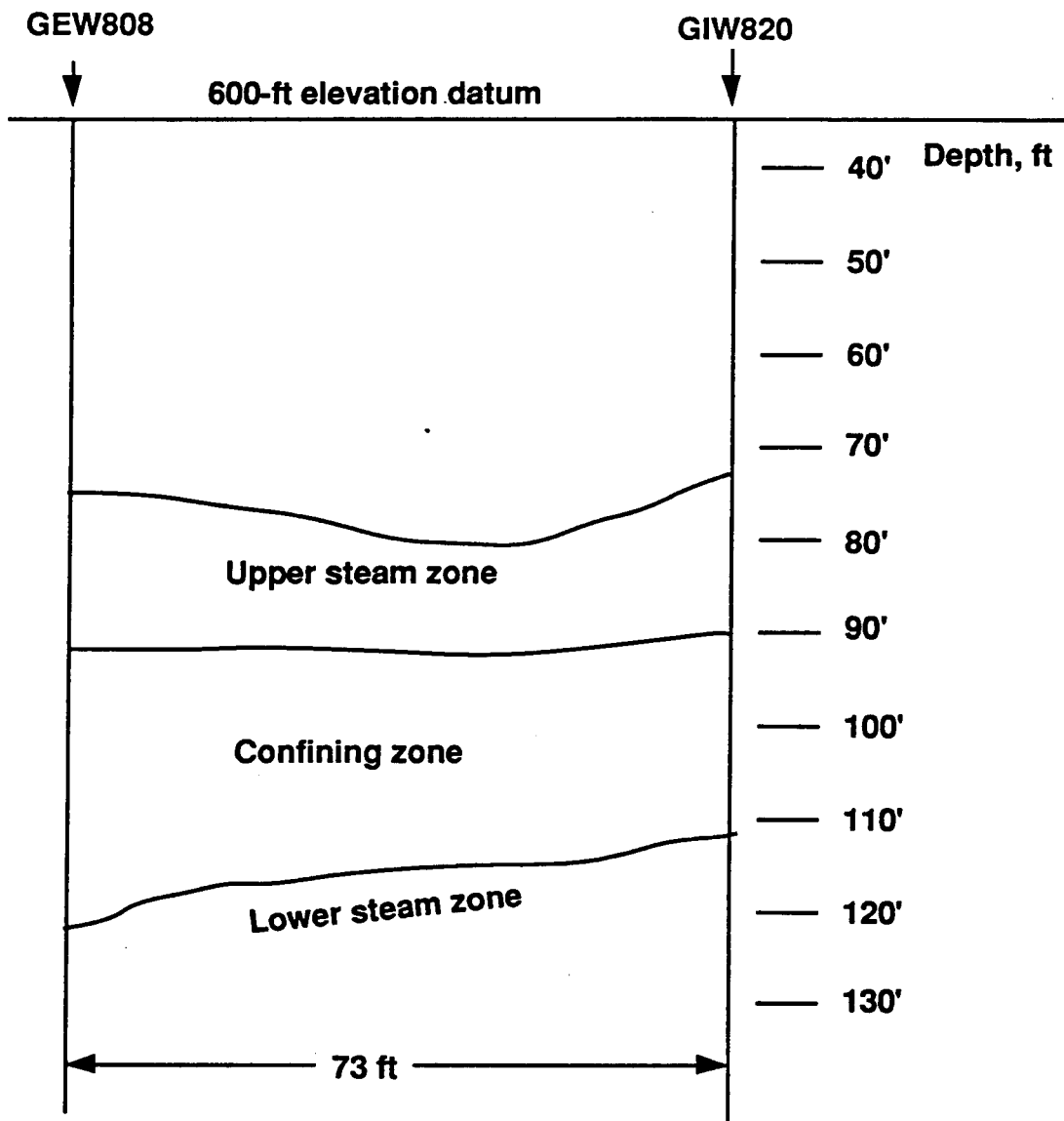


Figure 13. Cross section showing the simplified geology between well GIW820 and GEW808, one of the central extraction wells. Flow of air injected into the lower steam zone of GIW820 will be controlled by slope of the base of the confining zone (clay aquitard).

Table 2. Tracer gas analysis from the first sparging application.

Wells	Date	Time	22Ne/20Ne	Flow rate (scfm)
Injection Well	11/16/93	8:52	0.364	55.0
	11/16/93	9:15	0.368	53.5
	11/16/93	10:17	0.370	53.5
	11/16/93	15:23	0.365	54.0

	Date	Time	Elapsed time (h)	22Ne/20Ne	% injected air
ICE-in	11/16/93	10:41	2.0	0.102	0.0
	11/16/93	11:50	3.2	0.102	0.0
	11/16/93	12:34	3.8	0.125	8.6
	11/16/93	13:25	4.8	0.102	0.0
	11/16/93	13:57	5.3	0.103	0.4
	11/16/93	14:30	5.8	0.103	0.4
	11/16/93	14:59	6.3	0.106	1.5
	11/16/93	15:30	6.8	0.103	0.4
	11/16/93	15:55	7.3	0.110	3.0
	11/16/93	18:00	9.3	0.103	0.4
	11/16/93	20:00	11.3	0.103	0.4
	11/17/93	8:35	24.0	0.108	2.2
	GIW815L	11/16/93	9:35	1.9	0.102
11/16/93		10:00	2.3	0.104	0.8
11/16/93		10:48	3.1	0.330	86.7
11/16/93		11:18	3.6	0.361	98.5
11/16/93		12:05	4.4	0.367	100.8
11/16/93		13:00	5.3	0.367	100.8
11/16/93		14:00	6.3	0.365	100.0
11/16/93		15:00	7.3	0.248	55.5
GIW815U	11/16/93	15:56	8.3	0.140	14.4
	11/16/93	10:26	1.8	0.128	9.9
	11/16/93	11:30	2.8	0.116	5.3
	11/16/93	12:43	4.1	0.116	5.3
	11/16/93	13:43	5.1	0.114	4.6
	11/16/93	14:45	6.1	0.111	3.4
	11/16/93	15:45	7.1	0.112	3.8

used to get some indication of the relative amounts of injected air passing in that direction. Table 2 shows that the first trace of injected air was seen in the lower steam interval at GIW815 in the 10:00 a.m. sample. Thus, the total travel time for the air in the saturated zone between GIW820 and GIW815 (about 70 ft distance) was about 2.3 h. The amount of injected air detected in the lower interval of GIW815 reached 100% by 4.4 h into the sparging, with values dropping off to 55.5% just before air injection was stopped. This suggests that the flow path somehow became altered after about 6 h.

Table 2 shows that some of the injected air was also getting into the vadose zone, as shown by the tracer values obtained for the upper steam interval in GIW815. The initial value was the highest, with the percent of injected air decreasing gradually to about 4% after 7 h. The fact that tracer air reached the upper interval of GIW815 before it reached the lower interval suggests that the input air was getting into the vadose zone very quickly. Values of samples from the input to the ICE show rather erratic behavior. These samples probably represent air coming from the vadose zone. The first sample of injected air was detected after about 3.8 h, but subsequent samples showed very low to no injected air component for the next 2 h. A later peak at the ICE-in sample port of 3.0% injected air occurred after 7.3 h. A trace of injected air was still seen in the ICE-in the next morning, 24 h after injection began and more than 16 h after air injection ceased.

We also took samples of vapor for hydrocarbon chemistry analysis at the input to the ICE and in the lower steam interval of GIW815. These samples were taken in Tedlar bags using a vacuum pump and desiccator jar to inflate the bags (see Appendix 4 for details). Sampling for hydrocarbon chemistry was done at intervals similar to those for the trace gases. Table 3 shows the measured values of total petroleum hydrocarbons (TPH) (analysis up through the C₁₂ fraction), in ppmv. Because the flow rates from the input of the ICE are known, the mass extraction rate can be calculated, as shown in Table 3. The mass removal rate steadily increases until 6.3 h and then rapidly decreases. The TPH analyses for the samples from GIW815 cannot be interpreted in terms of mass removal because there is no flow in the well, but the data show a dramatic increase in the amount of hydrocarbons present after the first 2 h when the tracer gas data indicates that the vapor consists of 100% injected air. This suggests that the injected air is picking up a significant amount of hydrocarbons along its path in the saturated zone between GIW820 and GIW815.

The ERT difference images taken during the sparging are shown in Figure 14. Each image in Figure 14 shows the difference, between measurements taken at different times, in subsurface electrical resistivity over a cross section between two wells. The section TEP10–TEP6 (Fig. 11) runs almost parallel to the direction between GIW820 and the extraction wells. The section TEP10–TEP5 runs almost due north-south and at about 60° to the TEP10–TEP6 section. Section TEP5–TEP6 runs northwest-southeast and completes the triangle of the three wells. The lower two images show differences along section TEP10–TEP6 for measurements taken between 9:30 a.m. and 10:22 a.m. (left), and images taken between 9:30 a.m. and 12:57 p.m. (right), while air was being injected into GIW820 between depths of 112 to 132 ft. There is not much to be seen after only 1 h (lower left image), but after 3 h of air injection, resistivity increases about 0.5 ohm-m (lower right image). The zone of increased resistivity is centered on the area of the lower steam zone interval of GIW820 and extends slightly upward and toward the northeast (to the right in the cross section). This agrees with our intuition and modeling that indicated that the

Table 3. Hydrocarbon chemistry and cumulative mass removal during the first sparging application.

	Elapsed time (h)	Flow rate (scfm)	TPH (mg/L)	Total mass removal (g)	Mass removal rate (g/h)	Cumulative mass removal (g)	Cumulative mass removal (gal)
ICE	1.0	101	0.7	120	120	120.12	0.04
	1.8	101	4.7	672	806	792.19	0.26
	2.8	102	5.7	988	988	1,779.96	0.59
	4.3	106	3.8	1,027	684	2,806.46	0.94
	5.3	106	5.4	972	972	3,778.94	1.26
	6.3	106	6.9	1,243	1,243	5,021.55	1.67
	7.3	106	2.9	522	522	5,543.80	1.85
	9.3	101	1.1	378	189	5,921.31	1.97
	11.3	101	2.1	721	360	6,642.00	2.21
	13.3	101	1.6	549	275	7,191.10	2.40
	16.3	101	1.9	978	326	8,169.19	2.72
	19.3	101	0	0	0	8,169.19	2.72
	23.3	101	0.9	618	154	8,786.92	2.93
	GIW815-L	1.0	5	0.01			
1.3				(1% tracer recovered at GIW815-lower)			
1.8		5	4.0				
2.3				(100% tracer recovered at GIW815-lower)			
3.0				(6% tracer recovered at GIW815-upper)			
3.3		5	5.8				
4.3		5	21.0				
5.3		5	23.0				
6.3	5	20.0					

November 16 differences

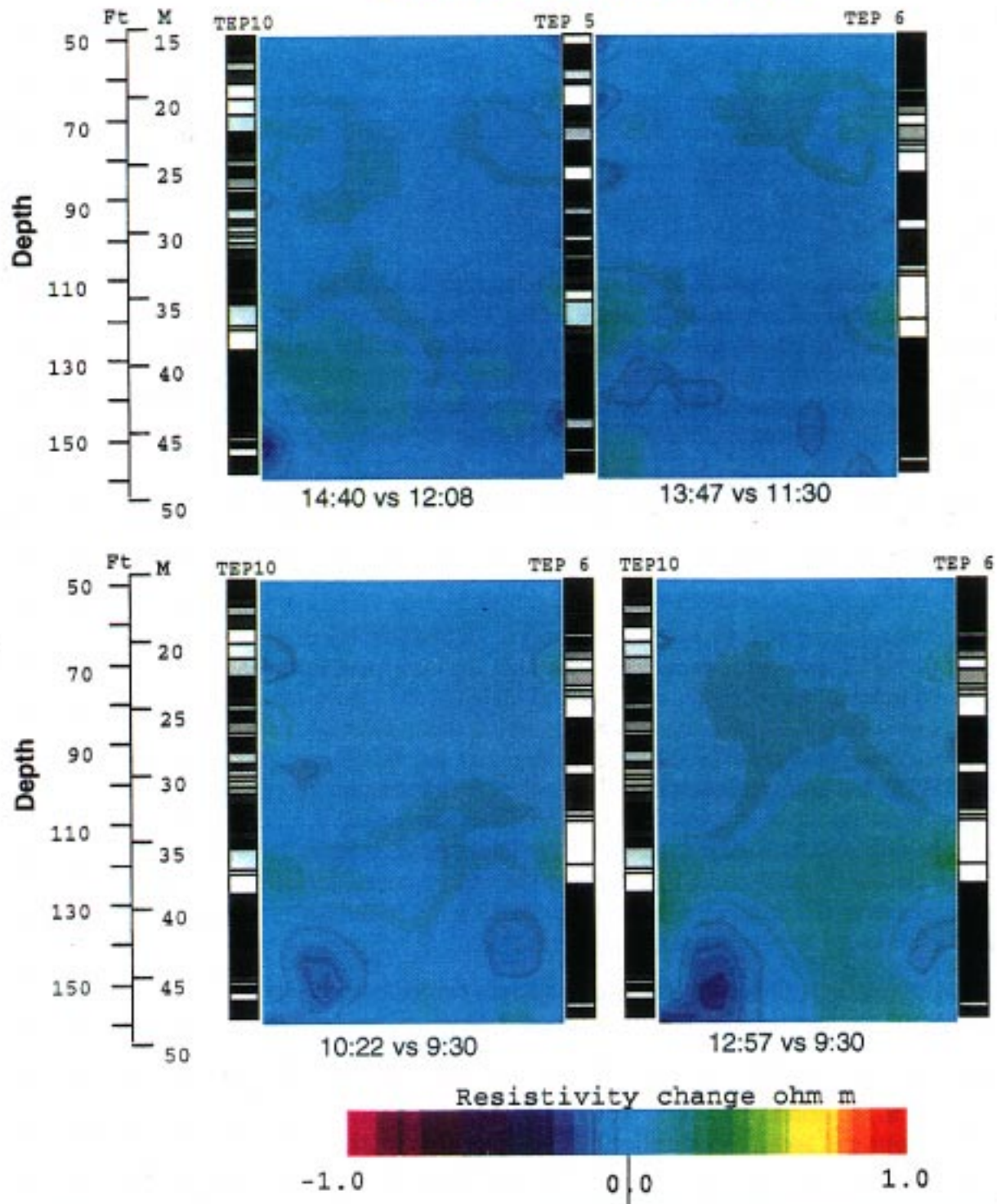


Figure 14. Electrical resistance tomography (ERT) images made from data taken during the first air sparging application. Refer to text for explanation of each part of the figure.

injected air (which will tend to dry the formation and increase the resistivity) will move upward and to the east. The upper two images, TEP10-TEP5 (left) and TEP5-TEP6 (right), do not show any definitive changes due to air injection. The zone of slightly enhanced resistivity near TEP10 on the upper left image, which occurs in the saturated zone, is probably not due to the flow of injected air, because the tracer data suggest that only a small amount of injected air went toward the extraction wells and that air was probably in the vadose zone. The TEP10-TEP6 image on the lower right, however, suggests that ERT imagery may be useful for tracking injected air. If the difference image were done over a longer time interval, the assessment of usefulness could be more definitive.

Air Sparging II

The first air sparging application was terminated after 7.3 h of air injection because we had confirmed that most of the injected air was not being recovered by the extraction wells. Movement of the injected air was controlled by buoyancy and by the slope of the base of the confining clay layer. The first sparging also indicated that injected air easily reached monitor well GIW815, located about 70 ft to the southeast of the injection well. For these reasons, we decided to use the lower steam interval of GIW815 as the injection well and GIW820 as the extraction well for the second sparging application. In order to establish stable background conditions, vacuum extraction was switched from the central extraction wells to GIW820 on November 18, continuing through the weekend. Because we were now extracting vapor from only one well instead of three, the extraction rate at the input to the ICE dropped from 101 scfm to about 47 scfm.

Air injection started at 8:49 a.m. on November 22 with air injection into the lower steam interval of GIW815, and vapor extraction from both the upper and lower intervals of GIW820. The screened interval in the lower steam zone of GIW820 is in the saturated zone; thus, almost all of the flow in GIW820 was coming from the upper steam zone (located in the vadose zone). Initial air injection pressures at GIW815 were about one psi; this suggested that the lower steam zone of GIW815 had been desaturated and that we were injecting air into the vadose zone. After completion of the injection, the water level in GIW815 was tagged at a depth of 119 ft. This is 7 ft below the top of the screened interval for the lower steam zone in the well, confirming that most of the air had probably been injected into the vadose zone. Initial injected air flow rates were estimated from the in-line gauges to be about 35 scfm, while analysis of the trace gas data suggested a somewhat higher rate of about 45 scfm.

We had originally intended for this sparging to run continuously for several days. However, the schedule for the start-up of the electrical heating operation required that initial testing of the electrical system had to begin on the evening of November 22, so we chose to shut down the air sparging operation between 3:30 p.m. and 9:00 p.m. on November 22 while vapor extraction was switched back to the central extraction wells. At 9:00 p.m., vapor extraction was switched back to GIW820 upper and lower and air injection continued overnight. At 10:00 a.m. the next day, we discovered that the air compressor had run out of fuel and had shut down some time between 9:00 a.m. and 10:00 a.m. The air compressor was refueled and restarted at 11:00 a.m., and air injection continued until 3:15 p.m. when we shut down sparging operations in order to prepare the TFF site for operational shutdown over the Thanksgiving holiday. The overall total time of air injection for this application was about 22.5 h.

The trace gas composition used was ^{22}Ne , 0.68%; ^{86}Kr , 0.085%; ^{136}Xe , 0.004%; and air, 99.23%. Note that both the particular isotope and percentage of Kr and Xe are different from those of the first application. Again, the trace gas mixture was injected into the input air stream at a rate of 1.0 L (STP)/min. As of this date, only the Ne ratios have been analyzed. Measured values of the $^{22}\text{Ne}/^{20}\text{Ne}$ ratio at the input to GIW815 (Table 4) ranged from 0.39 to 0.46, giving (from Fig. 12) an air injection rate of 51 to 40 scfm; again, a slightly higher value than indicated by the calibrated differential pressure measurement.

We did not use a monitoring well as we did in the first application. We took samples of the injected air at the input to GIW815, from the upper (85- to 105-ft depth) and lower (112 to 132 ft) screened intervals of GIW820, and from the input to the ICE (which represents the combined flow of the upper and lower intervals of GIW820) at 30- to 60-min intervals (Table 5). As Table 4 shows, because of the lower injection pressure in GIW815, it was more difficult to closely regulate the flow rate and the rate varied more widely than it did for the previous sparging. The $^{22}\text{Ne}/^{20}\text{Ne}$ ratio for background air, as measured just before the start of sparging, was 0.104. As shown in Figure 15, values of the percent injected air calculated from the $^{22}\text{Ne}/^{20}\text{Ne}$ ratio of the trace gas measured at the ICE-in and at the GIW820 upper interval track very closely. This confirms that almost all of the flow in GIW820 was coming from the upper interval. The data also indicate that the first trace of injected air arrived at the extraction well some time between 9:22 a.m. and 9:51 a.m., giving a travel time for the injected air of 33 to 62 min. This is significantly shorter than the travel time for the previous case, probably because the air in this case was moving primarily in the vadose zone. The percentage of recovered air in GIW820 upper reached a maximum of about 44% after about 6 h of air injection and then stayed more or less constant. The percent injected air had dropped off to about 5% at the ICE-in by the morning of November 24, about 19 h after air injection had ceased.

The percentage of trace gas in the lower interval of GIW820 is much more difficult to interpret. The first sample taken at the GIW820 lower, at 9:22 a.m., showed that about 26% of the vapor present was from the injected air. This is surprising because a sample taken at the same time from the GIW820 upper showed no tracer air present. However, if part of the lower interval of GIW820 was unsaturated, then it is conceivable that some of the air could have reached the lower interval of GIW820 before the upper interval by traveling in the unsaturated portion of this zone. The values of trace gas present in GIW820 lower did not vary by much over the 5.5 h that measurements were taken.

During the course of this application, we discovered that there was a problem with the way vapor samples were obtained in the field using the Tedlar bags. The problem first came to light when we took the initial vapor samples for hydrocarbon analyses at the beginning of air injection. Measured values for total hydrocarbons (TH) came in lower than 1,000 ppmv; these were significantly lower than what had been obtained several days earlier (values around 5,000 ppmv). We then had three different technicians each take a sample from the ICE-in, using the same procedure to fill the Tedlar bag, with all samples taken within about 10 min. The TH values for these three samples came out to be 70, 225, and 1,120 ppmv. This range of error was clearly due to problems with the sampling procedure. The problem was later identified as being due to ambient air getting into the sample bag because of poor connections with the sampling hose that goes to the vapor flow line. Addition of ambient air to the sample dilutes the results and makes the hydrocarbon content come out too low. The sampling procedures were revised to

Table 4. Composition of tracer gas during the second air sparging application.

	Date	Time	22Ne/20Ne	Flow rate (scfm)	
Injection well	11/22/93	9:12	0.388	51	
	11/22/93	10:12	0.427	44.5	
	11/22/93	10:55	0.405	48	
	11/22/93	11:53	0.41	47	
	11/22/93	14:58	0.416	46	
	11/23/93	13:57	0.462	40	
	11/23/93	15:05	0.459	41	
	Date	Time	Elapsed time (h)	22Ne/20Ne	% Injected air
ICE-in	11/22/93	9:54	1.0	0.120	5.6
	11/22/93	11:09	2.4	0.185	26.9
	11/22/93	12:05	3.3	0.210	34.6
	11/22/93	13:03	4.3	0.223	38.9
	11/22/93	14:57	6.2	0.240	43.6
	11/22/93	16:29	7.7	0.234	42.5
	11/22/93	20:23	11.6	0.244	45.8
	11/22/93	23:41	14.7	0.230	41.2
	11/23/93	10:27	25.7	0.220	37.9
	11/23/93	14:02	29.2	0.254	42.1
	11/23/93	15:08	30.3	0.254	42.1
GIW820 upper	11/24/93	8:08	47.3	0.118	3.9
	11/22/93	9:22	0.6	0.104	0.0
	11/22/93	9:51	1.0	0.118	4.3
	11/22/93	10:25	1.6	0.154	16.3
	11/22/93	10:59	2.2	0.175	23.2
	11/22/93	11:35	2.8	0.201	31.7
	11/22/93	12:01	3.2	0.210	34.6
	11/22/93	12:26	3.6	0.219	37.6
GIW820 lower	11/22/93	12:56	4.1	0.225	38.3
	11/22/93	13:29	4.7	0.231	40.2
	11/22/93	14:35	5.8	0.241	43.4
	11/22/93	9:22	0.6	0.185	28.3
	11/22/93	9:51	1.0	0.188	25.8
	11/22/93	10:25	1.6	0.205	33.0
	11/22/93	11:43	2.9	0.175	23.2
	11/22/93	12:26	3.6	0.208	34.0
	11/22/93	13:29	4.7	0.186	26.8
	11/22/93	14:55	6.1	0.187	26.3

Table 5. TPH composition from canisters (trace gas samples), second sparging application.

Elapsed time (h)	ICE flow rate (scfm)	GIW820U TPH (ppmv)	ICE-in TPH (ppmv)	TPH (mg/L) @ STP	Total mass removal (g)	Mass removal rate (g/h)	Cumulative mass removal (g)	Cumulative mass removal (gal)	Sample from
1.0	48	4,868	-	17.15	1,398	1,398	1,398.38	0.47	GIW820U
1.1	48	-	4,290	15.11	123	1,232	1,521.61	0.51	ICE-in
2.2	49	6,066	-	21.37	1,957	1,779	3,478.31	1.16	GIW820U
2.3	49	-	4,340	15.29	127	1,273	3,605.58	1.20	ICE-in
3.2	49	4,171	-	14.69	1,101	1,223	4,706.39	1.57	GIW820U
3.3	49	-	4,430	15.60	130	1,299	4,836.30	1.61	ICE-in
4.1	48	4,355	-	15.34	1,001	1,251	5,837.11	1.95	GIW820U
4.2	48	-	4,550	16.03	131	1,307	5,967.81	1.99	ICE-in
4.7	48	3,618	-	12.74	520	1,039	6,487.47	2.16	GIW820U
6.1	47	-	3,860	13.60	1,520	1,086	8,007.48	2.67	ICE-in

eliminate this problem (see Appendix 4), but by the time this was accomplished we were already about 4 h into the air sparging application. As a consequence, the most important part of the hydrocarbon data for this application had been compromised.

However, we could still obtain hydrocarbon data from the early part of the sparging by using a portion of the air sampled for the noble gas tracers. Portions of gas from six samples each of the trace gas samples from the upper zone of GIW820 and from the ICE-in were transferred to smaller evacuated cylinders of known volume at a measured pressure. These samples (referred to here as the "canister" samples) were then analyzed for hydrocarbon chemistry in the same manner as the Tedlar bag samples. A comparison of the canister samples with the Tedlar bag can be seen from Table 6 and Figure 16. Figure 16 shows that, until the Tedlar bag sampling procedure was improved about 6 h after air injection began, the canister samples have consistently higher hydrocarbon concentrations than the Tedlar bag samples. The canister hydrocarbon concentrations show only a slight decrease with time as air sparging proceeds. Canister samples taken at the extraction wellhead (GIW820-upper) have slightly higher concentrations than those taken at similar times at the ICE-in. This suggests that some product is possibly condensing in the plumbing between GIW820 and the ICE-in. In general, there seems to be no correlation between the amount of injected air recovered in GIW820-upper and the hydrocarbon chemistry seen in the canister samples.

For the second sparging case, ERT profiles were run between wells TEP10-TEP6 (also used in the first sparging case), and TEP6-TEP1. The TEP10-TEP6 profile is nearly at right angles to and close to the upstream end of the path from GIW815 to GIW820. The TEP6-TEP1 profile lies parallel to the path between the injection and extraction well and about 20 ft to the west. The ERT difference images are shown in Figure 17. The two upper images are for the profile plane TEP10-TEP6. The one on the left is a difference image between 9:35 a.m. and 1:30 p.m. (4 h)

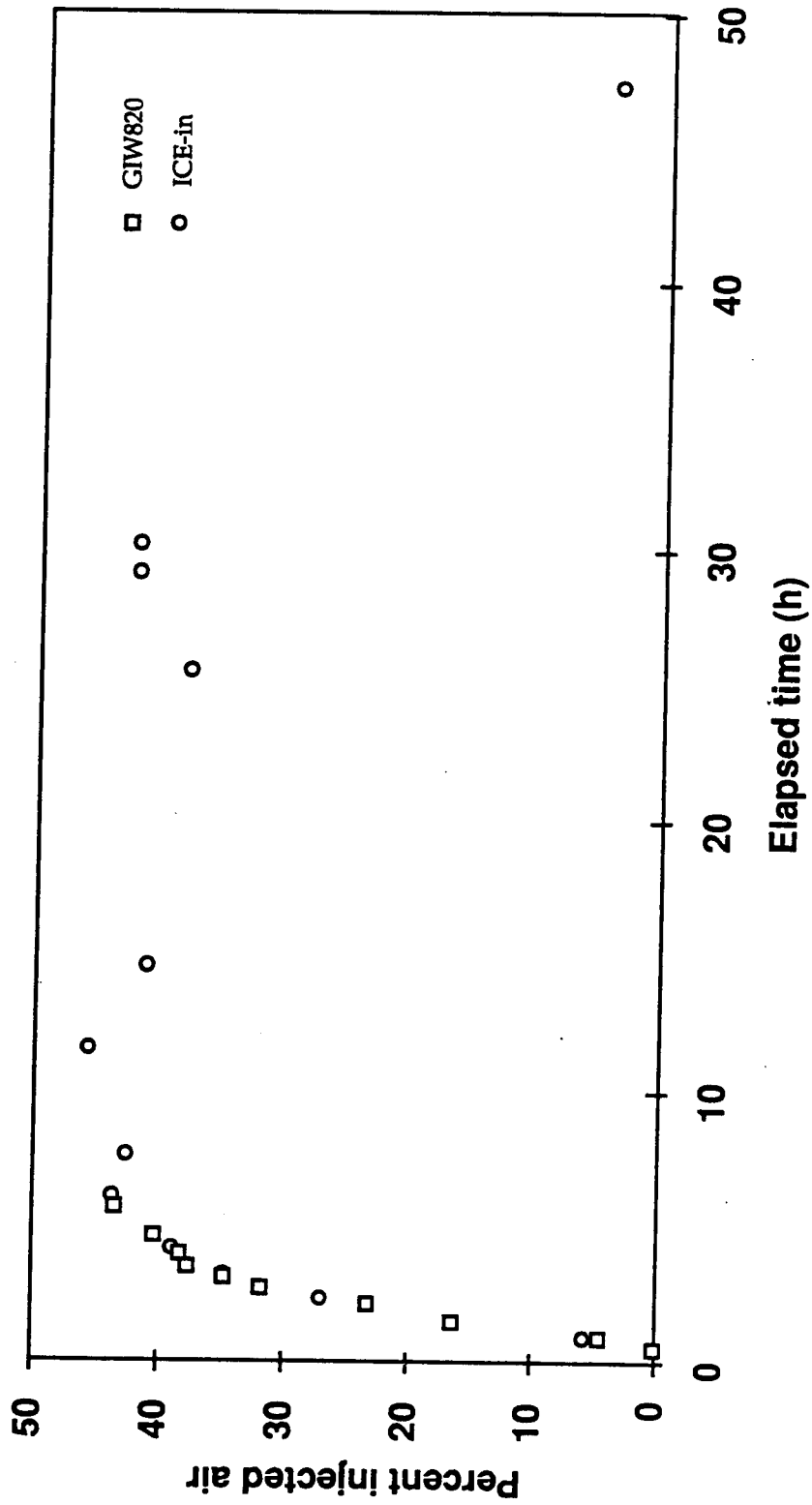


Figure 15. Percent injected air recovered at the upper interval of GIW820 and at the ICE-in versus elapsed time for the second sparging application. Percent injected air is determined from the $^{22}\text{Ne}/^{20}\text{Ne}$ ratio in the vapor samples.

Table 6. Hydrocarbon concentration data during the second sparging application.

Time of day	Elapsed time	Hydrocarbon chemistry and total petroleum hydrocarbons					
		TPH HC, (mg/L)	TPH HC (ppmV)	Tedlar bag ICE from GIW820	Canister sample ICE from GIW820	Tedlar bag GIW upper	Canister GIW upper
8:00	-0.67	18.5	5,261	-	-	-	5,261
8:40	-0.17	0.4	108	-	-	108	-
9:00	0.17	0.3	70	70	-	-	-
9:00	0.33	0.6	175	175	-	-	-
9:00	0.33	3.1	865	865	-	-	-
9:35	0.92	0.7	194	-	-	194	-
9:51	1.02	17.2	4,868	-	-	-	4,868
9:54	1.07	15.1	4,290	-	4,290	-	-
10:05	1.25	1.9	547	-	-	547	-
10:30	1.67	5.4	1,520	-	-	1,520	-
10:59	2.15	21.4	6,066	-	-	-	6,066
11:00	2.17	6.9	1,950	-	-	1,950	-
11:09	2.32	15.3	4,340	-	4,340	-	-
11:15	2.42	0.3	86	86	-	-	-
11:40	2.83	0.1	23	-	-	23	-
12:01	3.18	14.7	4,171	-	-	-	4,171
12:05	3.25	0.1	30	-	-	30	-
12:05	3.25	15.6	4,430	-	4,430	-	-
12:35	3.75	0.0	0	-	-	1	-
12:56	4.10	15.3	4,355	-	-	-	4,355
13:00	4.17	0.1	29	-	-	29	-
13:03	4.22	16.0	4,550	-	4,550	-	-
13:10	4.33	0.0	16	-	-	16	-
13:29	4.65	12.7	3,618	-	-	-	3,618
13:35	4.75	0.3	97	-	-	97	-
14:30	5.67	0.1	31	-	-	31	-
14:40	5.83	5.5	1,560	1,560	-	-	-
14:57	6.12	13.6	3,860	-	3,860	-	-
15:30	6.83	0.1	31	-	-	31	-
16:20	7.50	9.8	2,770	2,770	-	-	-
16:29	7.65	24.8	7,040	-	7,040	-	-
20:20	11.50	2.4	693	693	-	-	-
1:00	14.17	7.2	2,060	2,060	-	-	-
5:00	18.17	7.3	2,080	2,080	-	-	-
8:00	21.17	6.8	1,940	1,940	-	-	-
10:00	23.17	6.9	1,970	1,970	-	-	-
10:00	23.17	6.6	1,870	1,870	-	-	-
10:00	23.17	7.0	1,990	1,990	-	-	-
21:00	34.17	9.3	2,640	2,640	-	-	-
9:00	46.17	9.3	2,640	2,640	-	-	-

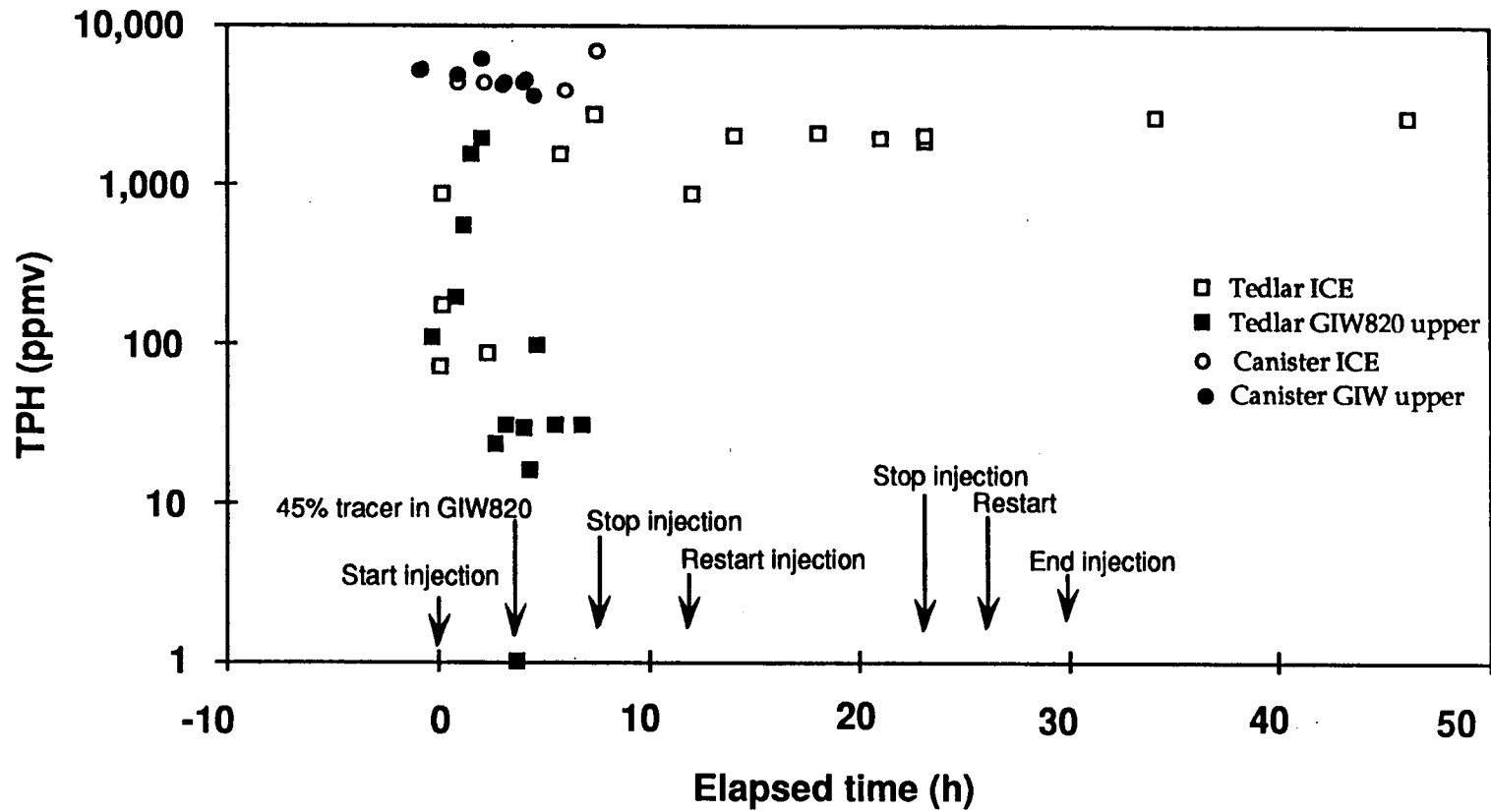


Figure 16. Hydrocarbon concentrations in vapor sampled during the second air sparging application. Canister samples are vapor samples originally taken for noble gas tracer analysis.

November 22-23 test

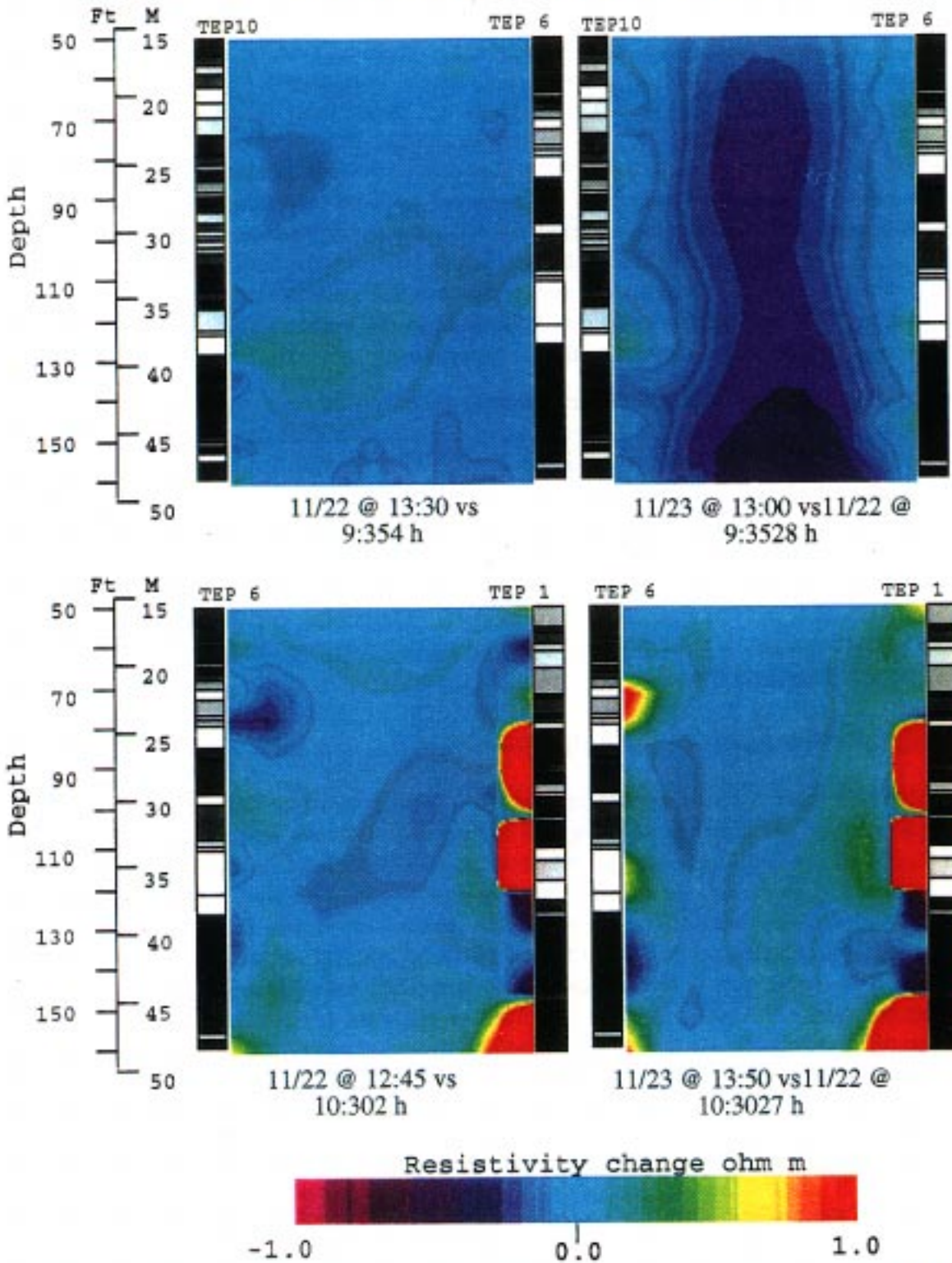


Figure 17. Electrical resistance tomography (ERT) images made from data taken during the second air sparging application. Refer to text for explanation of each part of the figure.

on November 22. The one on the right represents a longer interval of air injection, with 28 h difference in time for the image. The image on the left shows little to no effect of the air injection, even though by 1:30 p.m. at least 45% of the air recovered in GIW820-upper was injected air. The image on the top right of Figure 17 shows a decrease in resistivity of about 0.5 ohm-m over a very large vertical interval. This probably is caused by the movement of air upward in the vadose zone. The decrease in resistivity, rather than an increase as seen in the previous application, is puzzling. It may be due to the fact that most of the injected air was moving within the vadose zone in this case. Because relatively cold ambient air is being injected near the saturated zone, the air may pick up moisture as it mixes underground, taking more saturated air upward and causing the decrease in resistivity in the vadose zone. The two lower images in Figure 17 are difference images for the TEP6-TEP1 profile for images taken 2 h apart (left) and 27 h apart (right). The red zones appearing near TEP1 are caused by local anomalies in the electrodes in TEP1 and are not related to conditions in the matrix. These two lower images do not show any obvious effects related to the air sparging.

In this application, flow rates of the injected air (determined from the trace gas analyses) ranged from 40 to 48 scfm while the flow rates at the extraction well (as measured at the ICE) were 47 to 49 scfm. The trace gas analysis indicates that after the first 2.5 h, more than 30%, and up to 45%, of the injected air was being recovered in GIW820. This means that 14 to 20 scfm of the air reaching the ICE after 2.5 h of injection was injected air. The hydrocarbon concentration in the extracted vapor changed very little during buildup and maximum recovery of injected air; thus, the injected air was not diluting the extracted air, implying that the injected air was picking up hydrocarbons as it moved through the formation. The slight decrease with time in the hydrocarbon concentration in the extract vapor suggests that this contribution from the injected air did slightly decrease over time.

Summary of the Sparging Applications

Even with the interrupted schedule and problems with hydrocarbon sampling, the two sparging applications are considered a success because of what we learned from them. The ability to track the movement of the injected air is critical, especially in areas like the TFF site where the geology is extremely heterogeneous. In both cases, we found that noble gas tracer analysis is very useful for determining (1) where the injected air moves and how long it takes it to get there, (2) what fraction of the vapor is composed of injected air, and (3) the flow rate of injected air. The noble gas tracer samples also provided us with a valuable backup for hydrocarbon chemistry analysis. These capabilities of the trace gas analysis are only the first-order portion of the analysis. By analyzing the behavior of isotopes of gases with different mass (such as xenon or krypton), additional information can be gleaned, such as how much of the injected air actually contacted the water, what was its residence time, etc. We did not have time during this project to complete analyses of the other trace gas species or analyses of the water samples mentioned above.

Knowledge of the underground geological structure and the configuration of the water table is also important. These factors affect how the air will move and whether it is affecting the saturated or unsaturated zone. In areas of heterogeneous geology like the TFF site, however, it is not possible to know the subsurface geology well enough to predict in detail how the air will move. For example, fractures or inhomogeneities can provide pathways for air into the vadose

zone through an apparently impermeable formation, leading to travel pathways that are impossible to decipher. Computer simulations provide a valuable means to test conceptual ideas about subsurface conditions and study the efficacy of different extraction/injection well configurations. In our experience here, we found the computer simulations to be quite accurate in describing the general behavior of the injected air.

The ERT imagery used here can best be described as showing promise. The sparging times were not long enough to develop clear-cut changes in the formation that could be strongly reflected in the ERT imagery. In spite of these limitations, the images did suggest that changes as small as 0.5 ohm-m can be detected under good conditions. Our conclusion is that ERT imagery, in conditions like the TFF site, might be useful for tracking air movement in air sparging. However, for most applications, it will be very difficult to justify the expense of putting in dedicated wells for the sole use of obtaining ERT images for an air sparging operation.